Eur Spine J (2010) 19:1585–1595
DOI 10.1007/s00586-010-1386-x

ORIGINAL ARTICLE

A probabilistic finite element analysis of the stresses in the augmented vertebral body after vertebroplasty

Antonius Rohlmann · Hadi Nabil Boustani · Georg Bergmann · Thomas Zander

Received: 6 July 2009 / Revised: 5 March 2010 / Accepted: 9 March 2010 / Published online: 2 April 2010

Abstract Fractured vertebral bodies are often stabilized by vertebroplasty. Several parameters, including fracture type, cement filling shape, cement volume, elastic moduli of cement, cancellous bone and fractured region, may all affect the stresses in the augmented vertebral body and in bone cement. The aim of this study was to determine numerically the effects of these input parameters on the stresses caused. In a probabilistic finite element study, an osteoligamentous model of the lumbar spine was employed. Seven input parameters were simultaneously and randomly varied within appropriate limits for >110 combinations thereof. The maximum von Mises stresses in cancellous and cortical bone of the treated vertebral body L3 and in bone cement were calculated. The loading cases standing, flexion, extension, lateral bending, axial rotation and walking were simulated. In a subsequent sensitivity analysis, the coefficients of correlation and determination of the input parameters on the von Mises stresses were calculated. The loading case has a strong influence on the maximum von Mises stress. In cancellous bone, the median value of the maximum von Mises stresses for the different input parameter combinations varied between 1.5 (standing) and 4.5 MPa (flexion). The ranges of the stresses are large for all loading cases studied. Depending on the loading case, up to 69% of the maximum stress variation could be explained by the seven input parameters. The fracture shape and the elastic modulus of the fractured region have the highest influence. In cortical bone, the median values of the maximum von Mises stresses varied between 31.1 (standing) and 61.8 MPa (flexion). The seven input parameters could explain up to 80% of the stress variation here. It is the fracture shape, which has always the highest influence on the stress variation. In bone cement, the median value of the maximum von Mises stresses varied between 3.8 (standing) and 12.7 MPa (flexion). Up to 75% of the maximum stress variation in cement could be explained by the seven input parameters. Fracture shape, and the elastic moduli of bone cement and of the fracture region are those input parameters with the highest influence on the stress variation. In the model with no fracture, the maximum von Mises stresses are generally low. The present probabilistic and sensitivity study clearly showed that in vertebroplasty the maximum stresses in the augmented vertebral body and in bone cement depend mainly on the loading case and fracture shape. Elastic moduli of cement, fracture region and cancellous bone as well as cement volume have sometimes a moderate effect while number and symmetry of cement plugs have virtually no effect on the maximum stresses.

Keywords Lumbar spine · Vertebroplasty · Probabilistic · Sensitivity · Finite element analysis

A. Rohlmann (✉) · H. N. Boustani · G. Bergmann · T. Zander
Julius Wolff Institut, Charité-Universitätsmedizin Berlin, Augustenburger Platz 1, 13353 Berlin, Germany
e-mail: antonius.rohlmann@charite.de

Introduction

Fractured osteoporotic vertebral bodies are often stabilized by injection of bone cement into them. Two augmentation procedures, vertebroplasty and kyphoplasty, are those mainly used. In the case of vertebroplasty, acrylic bone cement is injected with high pressure into the marrow spaces of the collapsed vertebral body. The injection of bone cement is performed percutaneously through one or two injection cannulae. In kyphoplasty, an inflatable balloon tamp is first inserted percutaneously into the vertebral body.

When inflated with liquid, the balloon creates a cavity surrounded by compacted cancellous bone. After deflation, the cavity facilitates the controlled placement of bone cement with low risk of cement leakage [1]. Both procedures are performed under image guidance. Approximately 1–4 ml bone cement for each side can usually be inserted in vertebroplasty [2].

Blattert et al. [3] compared calcium phosphate (CaP) cement versus polymethylmethacrylate (PMMA) in a clinical trail of kyphoplasty. They observed radiographic signs of early cement fracture with subsequent fragmentation during the 6 weeks postoperative follow-up in 9 of 12 vertebral bodies with A3 type fracture (classification after Magerl et al. [4]) augmented with CaP. There was no case of cement failure, when PMMA had been used. Shin et al. [5] found progressive collapse of PMMA-augmented vertebra when an insufficient amount of cement was injected.

The effects of bone cement distribution and volume on vertebral stiffness after injection of bone cement has already been studied by several groups [6–10]. They found that vertebral stiffness and strength increase with higher bone cement volume and that only a small amount of bone cement is necessary in order to restore strength and stiffness. The stresses in the treated vertebral body after vertebroplasty, however, have not been investigated thoroughly. These are affected by several parameters, including type and severity of the fracture, amount and distribution of the injected cement, elastic modulus of cement and cancellous bone, and loading. Numerical deterministic studies about cement augmentation have been performed to determine influences of single parameters [10–17]. In these studies, one parameter was varied at a time while all of the others were kept constant. Combinations of extreme input values were not covered in such studies. However, it is just these combinations which may in fact lead to high stresses in bone and cement.

Keller et al. [17] studied the effects of cement augmentation using an axi-symmetric microstructural finite element model of a motion segment and bone damage scheme. Partial fill cement augmentation (15% of the total vertebral body volume) was effective in restoring the predamage stiffness only of slightly damaged segments. Their models also predicted that partial and complete fill cement augmentation alter bone stresses in the treated segment, disc stresses, and adjacent segment stresses.

The real distributions of bone cement were investigated by Chevalier et al. [15] in a numerical study. They studied the effects of different cement distribution and volume on vertebral body stiffness and strength. Cement distribution dominated the stiffening and strengthening effects of augmentation. Cement fillings that touched both endplates increased stiffness by up to 8 times and strength by up to 11 times, while fillings with cement touching only one endplate increased stiffness by up to only twice the original value, and only with a minimal increase in strength.

In probabilistic studies, the natural variations and uncertainties of several input parameters are incorporated into the model [18]. First, input parameters whose values are not exactly known as well as those which might affect the regarded results have to be identified and their probable range and distribution have to be specified. The values of each input parameter are sampled randomly according to the appropriate distribution [19]. Calculations are performed for a wide range of possible combinations, which allows one to discover parameter combinations that lead to unfavourable results with a reasonable number of designs. A probabilistic study delivers confidence limits providing an indication of the spread of the output parameters [19]. In a subsequent sensitivity analysis, the importance of the different input parameters can be calculated.

The effect of cement augmentation on the adjacent vertebrae is still a matter of debate. The new fractures often seen in these patients could be due to the natural history of the osteoporosis [20–22], due to the increased load caused by a wedge-shaped fracture [13], or due to the increased stiffness of the augmented vertebral body [11, 12, 23].

The aim of the present study was to determine in a probabilistic manner the effects of bone fracture shape, amount and distribution of bone cement as well as elastic modulus of bone cement, cancellous bone and fracture region on the von Mises stresses in the bone and cement after vertebroplasty. In a sensitivity analysis, we attempted to determine the relative importance of these parameters. The loading cases of standing, flexion, extension, lateral bending, axial rotation and walking were to be investigated.

Methods

Finite element model of intact lumbar spine

An osteoligamentous finite element model of the lumbar spine ranging from L1 vertebra to the disc L5/S1 was used (Fig. 1). This model has been validated with experimental data available like intervertebral rotations, intradiscal pressure and facet joint forces [24–27]. The geometry was taken from CTs. Eight-node hexahedral volume elements represented the five vertebrae and the ground substance of the intervertebral discs. The mesh was symmetric across the mid-sagittal plane. The vertebrae consisted of isotropic corticalis with a thickness of about 0.5 mm, transversely isotropic spongiosa with higher stiffness values in cranial/caudal direction, and the posterior structures (Table 1). The curved facet joints were only able to transmit compressive

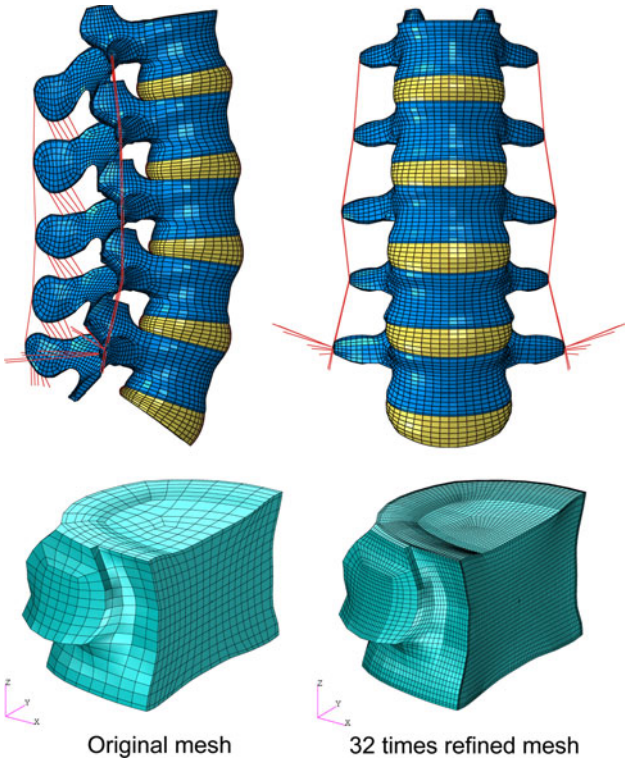

Fig. 1 Finite element model of the lumbar spine (*top*) and refined mesh of the submodel (*bottom right*)

forces. They had a thin cartilaginous layer and a gap of 0.5 mm [28]. The annuli fibrosi of the discs were modelled as fibre-reinforced hyperelastic composite [29]. The fibres were embedded in the ground substance in concentric rings around the nucleus. Cartilaginous endplates were also modelled. All major ligaments of the lumbar spine (anterior and posterior longitudinal ligament, ligamentum flavum, inter- and supraspinous ligaments, facet capsular ligaments, intertransverse ligaments and iliolumbar ligaments) were included in the model. They were represented by tension-only spring elements with non-linear material properties. The fibres and ligaments have been described in detail elsewhere [25, 30]. Material properties of the different tissues were taken from the literature (Table 1) [29, 31–33].

Fracture model

One A1 type fracture and five A3 type fractures (classification after Magerl et al. [4]) of the vertebral body L3 were investigated (Fig. 2). Fracture lines are based on X-rays of patients or roughly approximate published illustrations [4]. The increasing severity of the five A3 type fractures was modelled by adding additional fracture lines. It was assumed that the fracture reached till the cement. The fractures were simulated by reducing the elastic modulus of the corresponding elements representing cortical or cancellous bone. The stiffness of the fractured region in vivo is unknown. We assumed that it is lower than the average value for cancellous bone. Values between 5 and 75 MPa were chosen, which should cover the possible range. For two fracture models (No. 5 and No. 6, respectively), the cranial endplate and the cranial plus caudal endplates were also fractured.

Cement filling

Typical geometries and locations of the cement filling were chosen based on X-rays of many patients. The total amount of cement filling in the fractured L3 vertebra varied between 2 and 8 ml [2]. One or two cement plugs were assumed and the fillings were arranged symmetrically or unsymmetrically (Fig. 3). The bone cement was not in direct contact with the cranial and/or caudal vertebral endplate. In the finite element model, a perfect connection between cement and bone elements was assumed. The location and the shape of the cement plug were not explicitly varied.

Loading

The six loading cases standing, flexion, extension, lateral bending, axial rotation and walking were studied. Standing was simulated by applying a follower load [34, 35] of 500 N [36]. For simulating flexion, a follower load of 1,175 N and a flexion bending moment of 7.5 Nm were assumed [37]. For extension, lateral bending and axial

Table 1 Material properties and element types used for the different tissues of the intact model

Component	Elastic modulus (MPa)	Poisson ratio	Element type	References
Cortical bone	10,000	0.30	8-Node Hex	[44, 45]
Cancellous bone, healthy (transverse isotropic)	200/140	0.45/0.315	8-Node Hex	[33]
Posterior bony elements	3,500	0.25	8-Node Hex	[32]
Ground substance of annulus fibrosus	Hyperelastic, neo-Hookean $C_{10} = 0.3448$, $D_1 = 0.3$		8-Node Hex	[29]
Fibres of annulus fibrosus	Non-linear and dependent on the distance from the disc centre		Spring	[32]
Ligaments	Non-linear		Spring	[31, 46]
Cartilage of facet joint	Soft contact			[47]

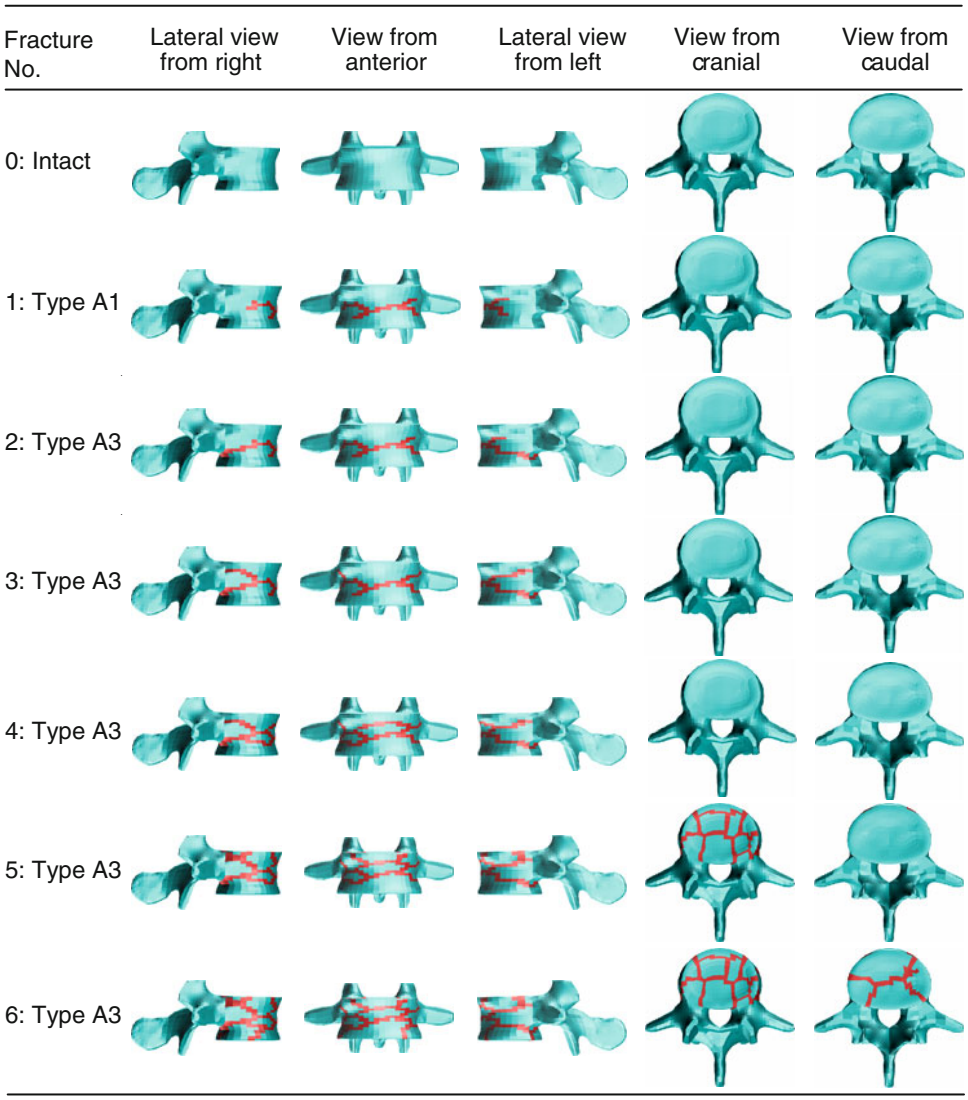

Fig. 2 Studied fracture shapes of the vertebra L3. *Red lines* represent fracture lines

rotation, a follower load of 500 N and a corresponding moment of 7.5 Nm were chosen. Walking causes an axial force which is about 30% higher than that for standing [38]. In addition, the spine is twisted during walking [39]. Thus, walking was simulated by applying a follower load of 650 N and a torsional moment of 7.5 Nm.

Probabilistic study

In this probabilistic study, the following seven input parameters were simultaneously randomized at vertebra L3 for each loading case.

1. Shape of the vertebral body fracture: beside the intact vertebral body, one A1 type fracture and five A3 type fractures were studied [4] (Fig. 2). A uniform distribution of the investigated fracture shapes was assumed (Table 2).
2. Amount of bone cement: volumes of 2, 4, 6, and 8 ml were studied. A uniform distribution of the four studied volumes was assumed (Fig. 3).
3. Number of cement fillings: one and two plugs were modelled. A uniform distribution was assumed.
4. Symmetry of cement fillings: symmetric and unsymmetric cement plugs were studied. A uniform distribution was assumed.
5. Elastic modulus of bone cement: the range was between 300 and 3,500 MPa with steps of 100 MPa. A uniform distribution was assumed (Table 2).
6. Elastic modulus of cancellous bone: a truncated Gaussian distribution with mean values of 100 MPa in axial direction and 70 MPa in transverse directions and a standard deviation of 50 MPa for axial direction was assumed. The range which was allowed was between 50 and 200 MPa for axial and between 35 and 140 MPa for transverse directions [33].

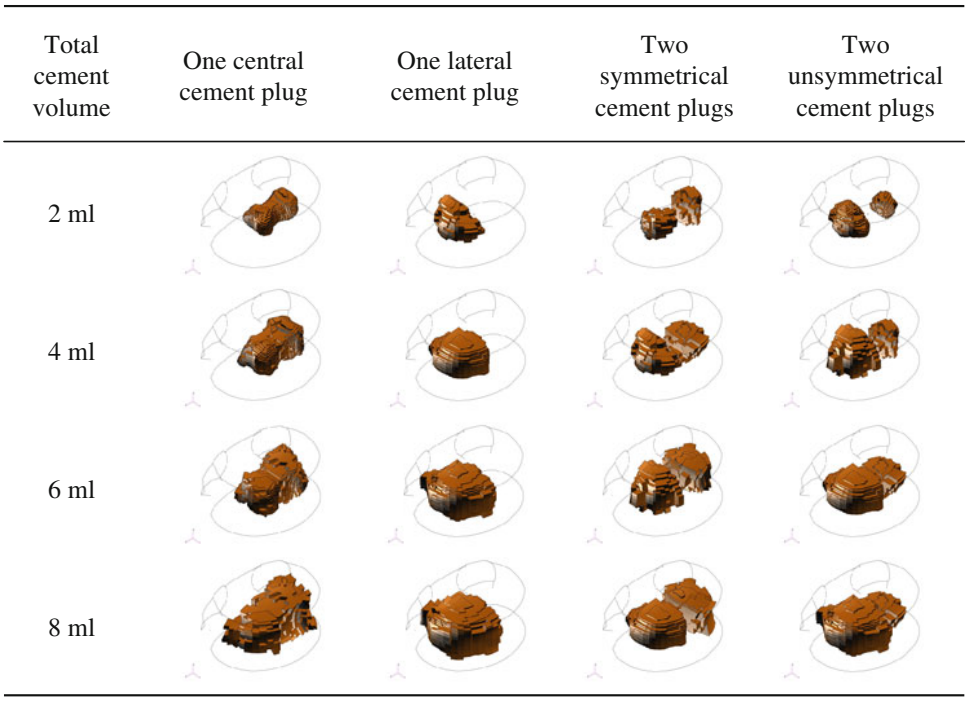

Fig. 3 Studied cement filling shapes

Table 2 Input parameters and their distribution

Input parameter	Distribution	Mean	SD	Minimum	Maximum	Steps
Fracture shape	Uniform			0	6	1
Cement volume	Uniform			2 ml	8 ml	2 ml
Number of cement blocks	Uniform			1	2	1
Symmetry of cement blocks	Uniform			0	1	1
Elastic modulus of cement	Uniform			300 MPa	3,500 MPa	100 MPa
Elastic modulus of cancellous bone (transverse isotropic)	Truncated Gaussian	100 MPa/ 70 MPa	50 MPa/ 35 MPa	50 MPa/ 35 MPa	200 MPa/ 140 MPa	1 MPa/ 0.7 MPa
Elastic modulus of fracture region	Truncated Gaussian	15 MPa	25 MPa	5 MPa	75 MPa	1 MPa

SD standard deviation

7. Elastic modulus of the fracture region: the range of the elastic modulus was between 5 and 75 MPa. A truncated Gaussian distribution with mean values of 15 MPa and a standard deviation of 25 MPa was assumed.

The Latin hypercube sampling method [40] was used to generate sample values of the input parameters. It is an advanced Monte Carlo simulation and a further development of the stratified sampling methodology. In comparison with the plain Monte Carlo simulation, Latin hypercube sampling requires fewer sampling points. The program optiSLang® (Dynardo, Weimar, Germany) was employed to randomize and calculate probabilistic results. In this study, >110 finite element calculations were performed for each of the six loading cases. The number of calculations was chosen to be sufficient for acceptable confidence intervals and a confidence level of 95%.

Output parameters of the probabilistic study were the maximum von Mises stresses in cancellous and cortical bone of the augmented vertebral body and in bone cement.

The finite element program ABAQUS, version 6.8 (SIMULIA Inc. Providence, RI, USA), was used with the pre- and post-processor PATRAN (Tata Technologies Europe Ltd, Stuttgart, Germany).

Submodel

In order to reduce calculation time, the submodelling technique was applied. First, the displacements and stresses were calculated for the complete lumbar model for each loading case. Then, the results for the displacements on the

caudal side of L3 vertebral body and the stresses on the cranial side of L3 vertebral body as well as on the cut face of the pedicles were applied to the submodel, which consists of the vertebral body of L3 (Fig. 1) with different fractures and cement augmentations. Tests showed that for these assumptions, the submodel delivers the closest results to those for the complete model. A convergence study showed the necessity of mesh refinement of the submodel. Thus, that mesh was refined by the factor of 32 when compared with the original mesh (Fig. 1).

Evaluation

The maximum von Mises stresses were evaluated for the cancellous and cortical bone of the vertebral body, and for bone cement. The von Mises stress was calculated at the elements' centres. It is a scalar and a measure of the overall stress at that point. Box plots were generated showing the median value, the interquartile range and the maximum and minimum values. The coefficient of determination is approximately the square of the linear correlation coefficient r, and gives the proportion of the variance of one variable that is predictable from the other variable. The linear coefficients of determination R^2 were calculated for the different input parameters as well as for the combination of all input parameters. The value for the combination of all input parameters is not simply the sum of the coefficients of the single parameters since the input parameters may indeed have an effect on each other.

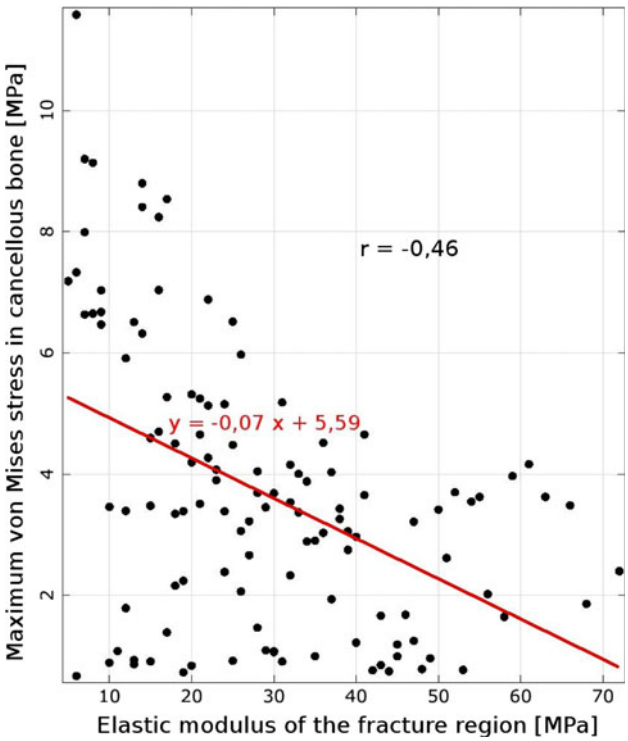

Fig. 4 Maximum von Mises stresses for several elastic moduli of the fracture region for lateral bending. Each *dot* represents the stress for a certain combination of input parameter. The linear regression curve including the equation as well as the correlation coefficient r are also given

Results

Cancellous bone

Figure 4 shows exemplarily the calculated maximum von Mises stresses in cancellous bone for all calculated conditions of input parameters for lateral bending as a function of different elastic moduli of the fracture region. Each dot represents a certain combination of input parameters. The linear regression line and the linear correlation coefficient are also provided. The maximum von Mises stress in cancellous bone decreases with increasing elastic modulus of the fracture region. Figures like this build the bases for subsequent analysis.

Box plots (Fig. 5) show the median values, the first and third quartile and the range of the maximum von Mises stress in the cancellous bone of the vertebra L3 for the various loading cases. The median value of the maximum stress for the different combinations of input parameters is lowest for standing (1.5 MPa) and highest for flexion (4.5 MPa). The ranges of the stresses are always large, especially for extension and flexion. The maximum peak values vary between 6.7 MPa for standing and 17.9 MPa for extension of the upper body. The lowest maximum stress (about 1 MPa) is similar for all loading cases.

Correlation coefficients r for linear and quadratic regression equations for the various input parameters and the different loading cases are given in Table 3. The quadratic value is equal to or slightly higher than the corresponding linear one. Correlation coefficients are only provided when $r \geq 0.4$ was calculated. For cancellous bone, this was the case only for fracture shape in combination with all loading cases as well as for elastic modulus of fracture region in combination with standing and lateral bending. The coefficients a and b of the linear and a, b and c of the quadratic regression lines are also provided in Table 3.

Coefficients of determination for the various input parameters and loading cases are given in Fig. 6. Between 63 (axial rotation) and 69% (extension) of the maximum stress variation could be explained by combinations of the seven input parameters. The fracture shape has always the highest influence on the variation of the maximum von Mises stresses. The highest coefficient of determination (44%) is calculated for extension as well as axial rotation. The elastic moduli of the fracture region and of cancellous

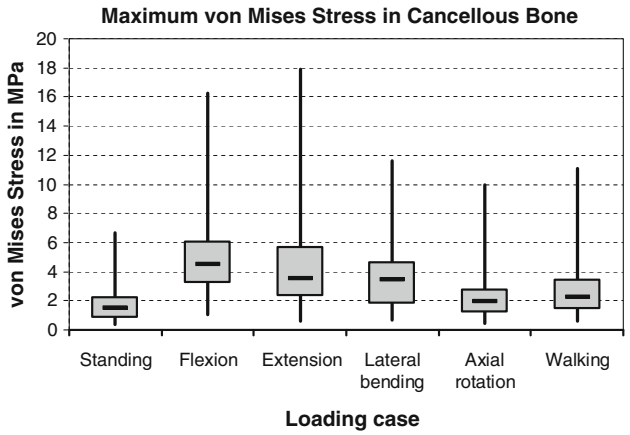

Fig. 5 Box plots comparing maximum von Mises stresses in cancellous bone of L3 for different loading cases. Median value, interquartile range, as well as maximum and minimum values for the calculated combinations of the seven input parameters are shown

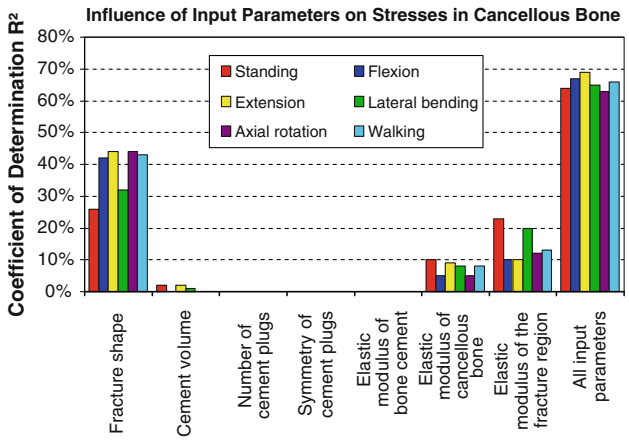

Fig. 6 Coefficients of determination of the different input parameters and loading cases for the stresses in cancellous bone

bone also consistently affect the results. Only for standing, lateral bending and extension did the cement volume have an effect on the stresses. The influences of number of cement plugs, symmetry of cement plugs and elastic modulus of bone cement on the maximum von Mises stresses in cancellous bone are always negligible.

Cortical bone

The maximum von Mises stress in cortical bone of the augmented vertebral body for each of the different loading cases are shown in Fig. 7. Also for cortical bone, the median value of the maximum stress is lowest for standing (31.3 MPa) and highest for flexion (61.8 MPa). The maximum peak value of 200.4 MPa is calculated for lateral bending of the upper body. The lowest maximum von Mises stress (about 13.1 MPa) is predicted for standing.

Table 4 provides the correlation coefficients r for linear and quadratic regression equations for those input parameters and loading cases where $r \geq 0.4$. This was the case only for fracture shape in combination with all loading cases studied. The coefficients of the linear and quadratic regression lines for these cases are also provided in Table 4.

Between 52 (axial rotation) and 80% (standing) of the maximum stress variation in cortical bone could be explained by the seven input parameters (Fig. 8). The fracture shape always has by far the strongest influence on the maximum von Mises stresses. The highest coefficient of determination (76%) is calculated for standing. The elastic modulus of the fracture region explains between 2 and 11% of the variance for standing, walking, axial rotation and extension. The influence of the other input parameters studied is for all loading cases <3%.

Table 3 Correlation coefficients r and coefficients a, b, and c of the linear and quadratic regression equations $y = ax + b$ and $y = ax^2 + bx + c$, respectively, for the correlation between the input parameters and the maximum stress in cancellous bone for various loading cases

Load case	Input parameter	Linear			Quadratic			
		r	a	b	r	a	b	c
Standing	Fracture shape	0.51	0.34	0.81	0.52	−0.04	0.58	0.61
	Elastic modulus of fracture region	−0.45	−0.04	2.95	0.55	0.00	−0.12	3.97
Flexion	Fracture shape	0.66	0.95	2.32	0.67	−0.11	1.60	1.79
Extension	Fracture shape	0.67	1.05	1.14	0.67	0.01	1.01	1.18
Lateral bending	Fracture shape	0.57	0.67	1.72	0.64	−0.20	1.84	0.75
	Elastic modulus of fracture region	−0.46	−0.07	5.59	0.54	0.00	−0.22	7.55
Axial rotation	Fracture shape	0.66	0.51	0.71	0.66	0.00	0.49	0.72
Walking	Fracture shape	0.66	0.56	0.94	0.66	−0.01	0.61	0.90

For the numerical equations, y is calculated in MPa and the x values correspond to the ranges given in Table 2. Values are shown only for $r \geq 0.4$

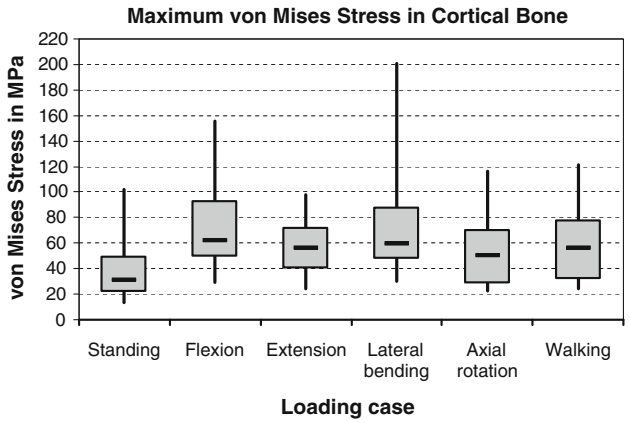

Fig. 7 Box plots comparing maximum von Mises stresses in cortical bone for different loading cases. Median value, first and third quartile, and the range of the stresses are shown for the studied combinations of input parameters

Bone cement

The median value of the maximum von Mises stress in bone cement is lowest for standing (3.8 MPa) and highest for flexion (12.7 MPa) (Fig. 9). The maximum peak value (39.1 MPa) is calculated for flexion of the upper body. The lowest maximum stress (about 1 MPa) is similar for all loading cases.

Correlation coefficients r for linear and quadratic regression equations as well as coefficients of the linear and quadratic regression lines for those input parameters and loading cases are given in Table 5 for those cases where r is ≥ 0.4. Correlation coefficients >0.5 are calculated only for fracture shape in combination with all loading cases as well as for cement volume in combination with lateral bending and for elastic modulus of cement in combination with standing.

Between 65 (extension) and 75% (lateral bending) of the maximum stress variation could be explained by the seven input parameters (Fig. 10). As for cancellous and cortical bone, the fracture shape always has the highest influence on the maximum von Mises stresses. The highest coefficient of determination (41%) is calculated for flexion. The elastic moduli of cement and fracture region as well always affect the results. The cement volume significantly affects the maximum von Mises stresses for all loading cases except standing, while the elastic modulus of cancellous bone is significant only for extension. The influence of number and symmetry of the cement plugs is always negligible.

In the intact model (fracture type 0) with cement, the calculated maximum von Mises stresses are generally low. Maximum values for cancellous and cortical bone and for bone cement are 1.7, 52.1 and 8.8 MPa, respectively.

Discussion

In this probabilistic and sensitivity study, von Mises stresses in cancellous and cortical bone of the augmented vertebral body and in bone cement were calculated after vertebroplasty for six loading cases. Of the seven input parameters studied, fracture shape has the strongest effect on the maximum stresses.

Despite the extensive finite element study, this study still has a few limitations. For the creation of the finite element models, several simplifications and assumptions were necessary. For example, the single trabeculae of the cancellous bone have not been modelled, which would be required to precisely estimate the fracture risk in a specific patient. Orthotropic homogeneous material was simulated instead, which is sufficient for general conclusions like those drawn in this study. The geometry of the lumbar spine was not varied in this study. The actual shape of the cement filling may be more filigree than in the model itself. The von Mises stress as a predictor of failure is generally

Table 4 Correlation coefficients r and coefficients a, b, and c of the linear and quadratic regression equations $y = ax + b$ and $y = ax^2 + bx + c$, respectively, for the correlation between the input parameters and the maximum stress in cortical bone for various loading cases

Load case	Input parameter	Linear			Quadratic			
		r	a	b	r	a	b	c
Standing	Fracture shape	**0.87**	8.24	11.40	**0.89**	0.84	3.17	15.7
Flexion	Fracture shape	0.74	12.14	38.79	0.79	2.65	−3.09	51.06
Extension	Fracture shape	0.77	7.42	34.7	**0.84**	−1.94	19.01	25.06
Lateral bending	Fracture shape	0.78	16.94	27.33	**0.85**	4.25	−8.24	48.21
Axial rotation	Fracture shape	0.63	8.30	28.16	0.63	−2.45	23.01	15.82
Walking	Fracture shape	0.67	8.76	31.46	0.74	−2.38	22.95	19.62

For the numerical equations, y is calculated in MPa and the x values correspond to the ranges given in Table 2. Values are shown only for $r \geq 0.4$

Bold values $r > 0.8$

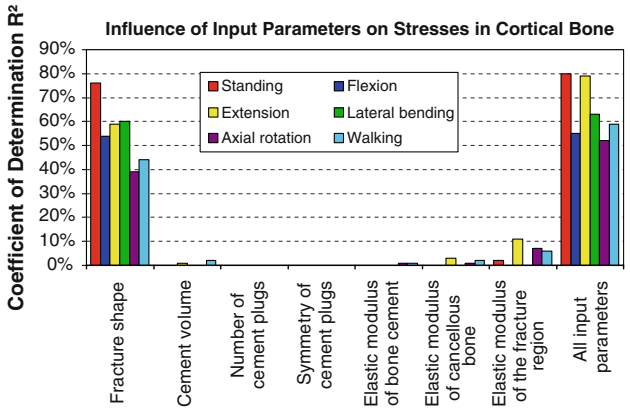

Fig. 8 Coefficients of determination of the different input parameters and loading cases for stresses in cortical bone

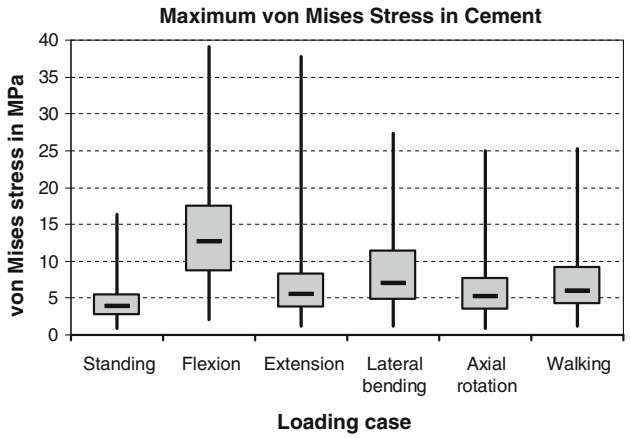

Fig. 9 Maximum von Mises stresses in bone cement for different loading cases and various input parameters. Median, first and third quartile, and the range are shown

used for isotropic ductile materials. Cancellous bone is neither isotropic nor ductile. Nevertheless, von Mises stress is often used to describe the stress situation in bone. Only 16 different cement filling shapes were studied, while there are infinite possibilities. No cement was assumed in the fracture gap outside the cement plug. The in vivo loading is more complex and had to be simplified for this study. After fracture, the vertebral bodies are often wedge-shaped. This shifts the centre of gravity of the upper body anteriorly, which increases the required muscle forces in an upright position and thus the spinal force [13]. This in turn increases the risk of a fracture in the adjacent vertebra. In the present study, the shape of the vertebral body was not changed when a fracture was assumed. These limitations affect the magnitude of the maximum stresses, which thus may not be very precise. The influences of the studied input parameters on the calculated maximum stresses, however, should be affected only slightly since the same assumptions have been made for all calculations.

A rigid bond was assumed between bone cement and cancellous bone. In vertebroplasty, bone cement enters into the space between the trabeculae and surrounds single trabeculae, which enables also the transfer of tensile forces at the interface. Thus, this assumption seems to be justified.

In the present study, the cement filling did not touch a bony endplate. In a previous unpublished study, very high stresses were predicted in the contact region when the cement was in contact with the vertebral endplate. The maximum von Mises stresses were 13 MPa in cancellous bone, 375 MPa in cortical bone and 190 MPa in cement. The corresponding maximum stresses in the present study are 18, 200, and 39 MPa, respectively. Chevalier et al. [15] measured a strong increase in stiffness and strength when the cement filling touched the endplates. Regions with high stiffnesses 'attract' the load and thus are higher stressed. The cortical shell of a vertebral body is much stiffer than the cancellous bone inside. The rigid bond between cement and bone allows the transfer of high shear stresses. Cements with low shear strength, like CaP cement, will most probably fail in these regions.

Bone cement in contact with bony endplates increases the stiffness of the augmented vertebra [15, 16, 41]. This leads to only small deformations of the endplates, a finding that not only results in high stresses in the augmented vertebrae but may also lead to high stresses in the endplate of the adjacent vertebra, which would increase the risk of an additional fracture. We recommend that bone cement be kept within the central region of the vertebral body and not come into contact with cortical bone.

The highest median of the maximum von Mises stresses are predicted for the loading case flexion. This is not surprising since the axial compressive load is also highest for this loading case. The maximum peak stress, however, was calculated in cancellous bone for the loading case extension (Fig. 5) and in cortical bone for the loading case lateral bending (Fig. 7).

The maximum stresses in cancellous and cortical bone and in bone cement do differ strongly but the strength of the different materials themselves also differ strongly. Cortical bone is much stronger than cancellous bone [42]. The strength of the cement filling depends on the composition of the cement. PMMA cement has as higher strength than e.g., CaP cement [3, 43].

The seven input parameter studied were able to explain between 52 (cortical bone, axial rotation) and 80% (cortical bone, standing) of the stress variation calculated. The remaining rest could probably be explained, e.g., by the geometry and position of the cement plugs, the shape of the fracture lines, or by nonlinear relationships between input and output parameters. These parameters are very difficult to include in a probabilistic study since they may vary strongly and are difficult to quantify. Fracture shape always has an

Table 5 Correlation coefficients r and coefficients a, b, and c of the linear and quadratic regression equations $y = ax + b$ and $y = ax^2 + bx + c$, respectively, for the correlation between the input parameters and the maximum stress in bone cement for various loading cases

Load case	Input parameter	Linear			Quadratic			
		r	a	b	r	a	b	c
Standing	Fracture shape	0.61	0.86	1.97	0.61	0.07	0.45	2.32
	Elastic modulus of cement	−0.42	0.12	2.20	0.42	−0.00	0.22	1.51
Flexion	Fracture shape	0.64	2.50	6.64	0.64	−0.16	3.44	5.88
Extension	Fracture shape	0.55	1.88	2.30	0.57	0.20	0.46	3.30
Lateral bending	Fracture shape	0.57	1.62	3.94	0.58	−0.19	2.73	3.02
	Cement volume	0.45	2.28	3.00	0.45	0.10	1.80	3.49
Axial rotation	Fracture shape	0.59	1.24	2.58	0.59	0.05	0.95	2.82
Walking	Fracture shape	0.62	1.40	3.01	0.62	0.09	0.90	3.43

For the numerical equations, y is calculated in MPa and the x values correspond to the ranges given in Table 2. Values are shown only for $r \geq 0.4$

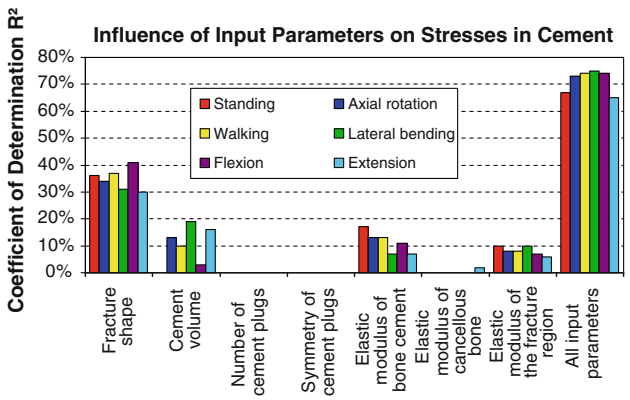

Fig. 10 Coefficients of determination of the different input parameters and loading cases for stresses in cement

effect on the maximum von Mises stresses. With increasing severity of the compression fracture, the number of fracture lines increases and thus the number of bony pieces of the vertebral body increases as well. If the cement volume is high, these bony pieces are connected by bone cement. The elastic modulus of the fracture region affects the maximum stresses in nearly all cases. This modulus is also a measure of the healing status of the vertebral body fracture and thus should increase with post-fracture time. This study shows that the maximum stresses are mainly influenced by the fracture shape and elastic modulus of fracture region. The other five input parameters together explain usually less than these two fracture parameters do.

More than 80% of all correlation coefficients were <0.4, which indicates a weak correlation. Values >0.4 were always calculated for fracture shape, and sporadic for elastic moduli of fracture region and cement.

This probabilistic and sensitivity study demonstrates clearly that the stresses in vertebral body and bone cement depend on several factors. The most important ones studied are loading case, fracture shape and elastic modulus of fracture region. However, even with the seven input parameters studied, only a part of the variance of the maximum von Mises stresses could be explained. A significant part of the remaining variance can most probably be explained by the geometry and position of the cement plugs, the shape of the fracture lines and by nonlinear relationships between input and output parameters.

Acknowledgments This study was financially supported by Heraeus Medical GmbH, Wehrheim, Germany and the Deutsche Forschungsgemeinschaft, Bonn, Germany (Ro 581/17-2). Finite element analyses were performed at the Norddeutscher Verbund für Hoch-und Höchstleistungsrechnen (HLRN). The authors thank N.K. Burra for technical assistance.

References

1. Heini PF, Orler R (2004) Kyphoplasty for treatment of osteoporotic vertebral fractures. Eur Spine J 13:184–192
2. Garfin SR, Yuan HA, Reiley MA (2001) New technologies in spine: kyphoplasty and vertebroplasty for the treatment of painful osteoporotic compression fractures. Spine 26:1511–1515
3. Blattert TR, Jestaedt L, Weckbach A (2009) Suitability of a calcium phosphate cement in osteoporotic vertebral body fracture augmentation: a controlled, randomized, clinical trial of balloon kyphoplasty comparing calcium phosphate versus polymethylmethacrylate. Spine (Phila Pa 1976) 34:108–114
4. Magerl F, Aebi M, Gertzbein SD, Harms J, Nazarian S (1994) A comprehensive classification of thoracic and lumbar injuries. Eur Spine J 3:184–201
5. Shin DA, Kim KN, Shin HC, Kim SH, Yoon DH (2008) Progressive collapse of PMMA-augmented vertebra: a report of three cases. Zentralbl Neurochir 69:43–46
6. Belkoff SM, Mathis JM, Jasper LE, Deramond H (2001) The biomechanics of vertebroplasty. The effect of cement volume on mechanical behavior. Spine 26:1537–1541
7. Liebschner MA, Rosenberg WS, Keaveny TM (2001) Effects of bone cement volume and distribution on vertebral stiffness after vertebroplasty. Spine 26:1547–1554
8. Molloy S, Mathis JM, Belkoff SM (2003) The effect of vertebral body percentage fill on mechanical behavior during percutaneous vertebroplasty. Spine 28:1549–1554

9. Rohlmann A, Zander T, Jony A, Weber U, Bergmann G (2005) Einfluss der Wirbelkörpersteifigkeit vor und nach Vertebroplastik auf den intradiskalen Druck. Biomed Tech (Berl) 50:148–152
10. Sun K, Liebschner MA (2004) Biomechanics of prophylactic vertebral reinforcement. Spine 29:1428–1435
11. Baroud G, Nemes J, Heini P, Steffen T (2003) Load shift of the intervertebral disc after a vertebroplasty: a finite-element study. Eur Spine J 12:421–426
12. Polikeit A, Nolte LP, Ferguson SJ (2003) The effect of cement augmentation on the load transfer in an osteoporotic functional spinal unit: finite-element analysis. Spine 28:991–996
13. Rohlmann A, Zander T, Bergmann G (2006) Spinal loads after osteoporotic vertebral fractures treated by vertebroplasty or kyphoplasty. Eur Spine J 15:1255–1264
14. Villarraga LM, Cripton PA, Bellezza AJ, Berlemann U, Kurtz SM, Edidin AA (2004) Knochen und Knochen-Zement-Belastungen in der thorakolumbalen Wirbelsäule nach Kyphoplastik. Eine Finite-Element-Studie. Orthopade 33:48–55
15. Chevalier Y, Pahr D, Charlebois M, Heini P, Schneider E, Zysset P (2008) Cement distribution, volume, and compliance in vertebroplasty: some answers from an anatomy-based nonlinear finite element study. Spine 33:1722–1730
16. Teo J, Wang SC, Teoh SH (2007) Preliminary study on biomechanics of vertebroplasty: a computational fluid dynamics and solid mechanics combined approach. Spine 32:1320–1328
17. Keller TS, Kosmopoulos V, Lieberman IH (2005) Vertebroplasty and kyphoplasty affect vertebral motion segment stiffness and stress distributions: a microstructural finite-element study. Spine 30:1258–1265
18. Haldar A, Mahadevan S (2000) Probability, reliability, and statistical methods in engineering design. Wiley, New York
19. Dar FH, Meakin JR, Aspden RM (2002) Statistical methods in finite element analysis. J Biomech 35:1155–1161
20. Ananthakrishnan D, Berven S, Deviren V, Cheng K, Lotz JC, Xu Z, Puttlitz CM (2005) The effect on anterior column loading due to different vertebral augmentation techniques. Clin Biomech (Bristol, Avon) 20:25–31
21. Davis JW, Grove JS, Wasnich RD, Ross PD (1999) Spatial relationships between prevalent and incident spine fractures. Bone 24:261–264
22. Jensen ME, Dion JE (2000) Percutaneous vertebroplasty in the treatment of osteoporotic compression fractures. Neuroimaging Clin N Am 10:547–568
23. Wilcox RK (2006) The biomechanical effect of vertebroplasty on the adjacent vertebral body: a finite element study. Proc Inst Mech Eng [H] 220:565–572
24. Zander T, Rohlmann A, Bock B, Bergmann G (2007) Biomechanische Konsequenzen von verschiedenen Positionierungen bewegungserhaltender Bandscheibenimplantate. Eine Finite-Elemente-Studie an der Lendenwirbelsäule. Orthopade 36:205–211
25. Zander T, Rohlmann A, Calisse J, Bergmann G (2001) Estimation of muscle forces in the lumbar spine during upper-body inclination. Clin Biomech 16:S73–S80
26. Rohlmann A, Bauer L, Zander T, Bergmann G, Wilke HJ (2006) Determination of trunk muscle forces for flexion and extension by using a validated finite element model of the lumbar spine and measured in vivo data. J Biomech 39:981–989
27. Zander T, Rohlmann A, Bergmann G (2009) Influence of different artificial disc kinematics on spine biomechanics. Clin Biomech (Bristol, Avon) 24:135–142
28. Rohlmann A, Zander T, Bock B, Bergmann G (2008) Effect of position and height of a mobile core type artificial disc on the biomechanical behaviour of the lumbar spine. Proc Inst Mech Eng [H] 222:229–239
29. Eberlein R, Holzapfel GA, Schulze-Bauer CAJ (2000) An anisotropic model for annulus tissue and enhanced finite element analysis of intact lumbar disc bodies. Comp Meth Biomech Biomed Eng 4:209–229
30. Rohlmann A, Zander T, Bergmann G (2005) Effect of total disc replacement with ProDisc on the biomechanical behavior of the lumbar spine. Spine 30:738–743
31. Nolte LP, Panjabi MM, Oxland TR (1990) Biomechanical properties of lumbar spinal ligaments. In: Heimke G, Soltesz U, Lee AJC (eds) Clinical implant materials, advances in biomaterials, vol 9. Elsevier, Heidelberg, pp 663–668
32. Shirazi-Adl A, Ahmed AM, Shrivastava SC (1986) Mechanical response of a lumbar motion segment in axial torque alone and combined with compression. Spine 11:914–927
33. Ueno K, Liu YK (1987) A three-dimensional nonlinear finite element model of lumbar intervertebral joint in torsion. J Biomech Eng 109:200–209
34. Patwardhan AG, Havey RM, Meade KP, Lee B, Dunlap B (1999) A follower load increases the load-carrying capacity of the lumbar spine in compression. Spine 24:1003–1009
35. Rohlmann A, Neller S, Claes L, Bergmann G, Wilke H-J (2001) Influence of a follower load on intradiscal pressure and intersegmental rotation of the lumbar spine. Spine 26:E557–E561
36. Rohlmann A, Zander T, Rao M, Bergmann G (2009) Applying a follower load delivers realistic results for simulating standing. J Biomech 42:1520–1526
37. Rohlmann A, Zander T, Rao M, Bergmann G (2009) Realistic loading conditions for upper body bending. J Biomech 42:884–890
38. Rohlmann A, Claes L, Bergmann G, Graichen F, Neef P, Wilke H-J (2001) Comparison of intradiscal pressures and spinal fixator loads for different body positions and exercises. Ergonomics 44:781–794
39. Rozumalski A, Schwartz MH, Wervey R, Swanson A, Dykes DC, Novacheck T (2008) The in vivo three-dimensional motion of the human lumbar spine during gait. Gait Posture 28:378–384
40. Gurdak JJ, McCray JE, Thyne G, Qi SL (2007) Latin hypercube approach to estimate uncertainty in ground water vulnerability. Ground Water 45:348–361
41. Hulme PA, Boyd SK, Heini PF, Ferguson SJ (2009) Differences in endplate deformation of the adjacent and augmented vertebra following cement augmentation. Eur Spine J 18:614–623
42. Fyhrie DP, Vashishth D (2000) Bone stiffness predicts strength similarly for human vertebral cancellous bone in compression and for cortical bone in tension. Bone 26:169–173
43. Ikenaga M, Hardouin P, Lemaitre J, Andrianjatovo H, Flautre B (1998) Biomechanical characterization of a biodegradable calcium phosphate hydraulic cement: a comparison with porous biphasic calcium phosphate ceramics. J Biomed Mater Res 40:139–144
44. Goel VK, Ramirez SA, Kong W, Gilbertson LG (1995) Cancellous bone Young's modulus variation within the vertebral body of a ligamentous lumbar spine—application of bone adaptive remodeling concepts. J Biomech Eng 117:266–271
45. Shirazi-Adl SA, Shrivastava SC, Ahmed AM (1984) Stress analysis of the lumbar disc-body unit in compression. A three-dimensional nonlinear finite element study. Spine 9:120–134
46. Rohlmann A, Zander T, Schmidt H, Wilke H-J, Bergmann G (2006) Analysis of the influence of disc degeneration on the mechanical behaviour of a lumbar motion segment using the finite element method. J Biomech 39:2484–2490
47. Sharma M, Langrana NA, Rodriguez J (1995) Role of ligaments and facets in lumbar spinal stability. Spine 20:887–900